Purification, Characterization, and Kinetics of Porcine Recombinant Dihydropyrimidine Dehydrogenase

ARTICLE *in* PROTEIN EXPRESSION AND PURIFICATION · AUGUST 1997

Impact Factor: 1.7 · DOI: 10.1006/prep.1997.0735 · Source: PubMed

PROTEIN EXPRESSION AND PURIFICATION **10,** 185–191 (1997)
ARTICLE NO. PT970735

Purification, Characterization, and Kinetics of Porcine Recombinant Dihydropyrimidine Dehydrogenase

Katrin Rosenbaum, Barbara Schaffrath, Wilfred R. Hagen,* Karin Jahnke, Frank J. Gonzalez,† Paul F. Cook,‡ and Klaus D. Schnackerz

*Physiologische Chemie I, Theodor-Boveri-Institut für Biowissenschaften, Universität Würzburg, Am Hubland, D-97074 Würzburg, Germany; *Department of Biochemistry, Agricultural University of Wageningen, NL-6703 HA Wageningen, The Netherlands; †Laboratory of Molecular Carcinogenesis, National Cancer Institute, Bethesda, Maryland 20892; and ‡Department of Chemistry and Biochemistry, University of Oklahoma, Norman, Oklahoma 73019*

Received November 4, 1996, and in revised form January 14, 1997

Porcine recombinant dihydropyrimidine dehydrogenase was purified from *Escherichia coli* cells using cell disruption, ammonium sulfate fractionation, and chromatography on DEAE-cellulose and 2′,5′-ADP–Sepharose. The yield was 60% with a specific activity of 14 units/mg protein. On SDS/PAGE the purified dehydrogenase exhibits a single band, indicating that no proteolytic degradation was taking place during purification. In agreement with the native enzyme, all cofactors, FMN, FAD, NADPH, and two iron–sulfur clusters, have been found. EPR spectra of the reduced dehydrogenase obtained at pH 9.5 are characteristic for two [4Fe–4S]$^{1+}$ cubanes in dipolar interaction. Quantification of the observed signals indicated 0.95 spins per subunit, showing only partially reduced iron–sulfur clusters. The kinetic parameters of the porcine recombinant enzyme are very similar to those of the native enzyme. Thus, it can be concluded that the porcine recombinant enzyme behaves like the native dehydrogenase.

Dihydropyrimidine dehydrogenase (EC 1.3.1.2; DPD)[1] is the first enzyme in the three-step degradation of uracil and thymine. In a strictly NADPH-dependent step, these pyrimidines are reduced to 5,6-dihydropyrimidines. After ring cleavage by dihydropyrimidine amidohydrolase, ammonium ions and CO_2 are formed in a reaction catalyzed by ureidopropionase, leaving as products β-alanine and β-aminoisobutyrate, respectively (1). 5-Fluorouracil, which is clinically used in cancer therapy, is likewise effectively and rapidly degraded to fluorinated products which are thought to cause multiple drug side effects in the nervous system (2). α-Fluoro-β-alanine was reported to be a neurotoxic agent (3). The inhibition of the degradative pyrimidine pathway could greatly potentiate the therapeutic effectiveness of 5-fluorouracil.

The main activity of DPD is found in liver, with minimal activity in the kidney, lung, pancreas, colon, and breast (4). The enzymes purified from rat (5), pig (6), bovine (7), and human (8) livers are composed of two identical subunits of M_r 107,000. The pig and human liver enzymes contain multiple flavins and iron–sulfur clusters (6,8).

The kinetic mechanism of the pig liver enzyme has been shown to be a nonclassical two-site ping-pong mechanism through initial velocity studies in the absence and presence of product and dead-end inhibitors (9). Separate binding sites are available for each substrate/product pair, NADPH/$NADP^+$ and uracil/5,6-dihydrouracil. Employing ^{1}H NMR spectroscopy and stereospecifically deuterated coenzymes, it could be shown that DPD from pig liver abstracts specifically the pro-*S* hydrogen of NADPH, making it a member of the B-side stereospecific class of dehydrogenases (10). The stereospecificity of the second-half reaction was studied by Gani and Young (11) by using β-alanine samples which were stereospecifically labeled in each of the four C–H bonds and ^{1}H NMR spectroscopy. It was shown that uracil is reduced with overall *anti*-addition of the hydrogen at the *si* face of C-6 and at the *si* face of C-5.

Isotope-effect and pH-rate data suggest a rate-determining reductive first-half reaction in which the reduction of the flavin by NADPH has only a minor rate

[1] Abbreviations used: DPD, dihydropyrimidine dehydrogenase; DTT, dithiothreitol; EPR, electron paramagnetic resonance spectroscopy; IPTG, isopropyl thiogalactopyranoside; PMSF, phenylmethylsulfonyl fluoride; 2,6-DHP, 2,6-dihydroxypyridine; DHU, 5,6-dihydrouracil; Ches, 2-(*N*-cyclohexylamino)ethanesulfonic acid.

1046-5928/97 $25.00

limitation, while the next step, protonation of the flavin at N-1, is slow. An enzymatic general acid with a p*K* of 8.2 is required to protonate N-1 of the flavin (12). In the second-half reaction, uracil is reduced at C-6 by flavin and protonated by an enzymatic general acid with a p*K* of 9. The hydride transfer from N-5 of the flavin to C-5 of uracil is facilitated by an enzymatic general base with a p*K* of 5.6, which accepts a proton from N-1 of the flavin (12). Electron transfer from site 1 (NADPH-binding site) to site 2 (uracil-binding site) presumably occurs via FeS clusters.

Although a mechanism has been proposed for DPD, a number of questions remain. Little is known about which flavin acts at what site, and how the iron–sulfur clusters facilitate the electron transfer. The cDNA of the pig and human liver DPD has been cloned and sequenced and the cDNA for pig liver DPD was expressed in *Escherichia coli* (13). The aim of this study is to report the purification of the porcine recombinant DPD from *E. coli* and the characterization of its physicochemical and kinetic parameters compared to the native enzyme.

MATERIALS AND METHODS

Chemicals. $NADP^+$ and NADPH were obtained from Boehringer Mannheim. Uracil, ATP-ribose, Mes, Mops, Ches, Tricine, D_2O, and dithiothreitol were purchased from Sigma, while 2,6-dihydroxypyridine was from Aldrich. All other chemicals were obtained from commercial sources and were of the highest purity available.

Enzyme assay. Enzyme activity was determined at 30°C by monitoring the decrease in absorbance at 340 nm as reported previously (9). A typical reaction mixture contained 100 mM potassium phosphate buffer, pH 7.3, 1.0 mM dithioerythritol, 60 μM NADPH, 50 μM uracil, and 2 units DPD in a final volume of 1 ml. The reaction was initiated with uracil and run against a blank containing the identical reaction mixture without uracil. One unit of enzyme activity is defined as the amount of enzyme that causes the disappearance of 1 μmol of NADPH/h.

General methods. Metal content, acid-labile sulfide, protein, flavin determination, and SDS/PAGE were carried out as reported previously (6). Native gel electrophoresis was performed on 4–20% gradient gels with BRL Mini V8 × 10 (Life Technologics, Inc.) using bovine serum albumin (67 kDa), lactate dehydrogenase (140 kDa), catalase (232 kDa), ferritin (440 kDa), and thyroglobin (669 kDa) as protein standards. The p*I* determination was accomplished on Phastgel IEF 3-9 and 4-6.5 (Pharmacia) with the Phast system (Pharmacia) using standard proteins. Gels were stained for protein with silver (14).

Data processing. Reciprocal initial velocities were plotted versus reciprocal substrate concentrations, and the experimental data were fitted using Eqs. [1]–[5] by a nonlinear least-squares method and the Fortran programs of Cleland (15).

$$v = VA/(K_a + A) \quad [1]$$

$$v = VA/(K_a(1 + I/K_{is}) + A) \quad [2]$$

$$v = VA/(K_a(1 + K_{is}) + A(1 + I/K_{ii})) \quad [3]$$

$$v = VA/(K_a + A(1 + I/K_{ii})) \quad [4]$$

$$\log Y = \log(C/1 + H/K_1 + K_2/H) \quad [5]$$

Substrate saturation curves were fitted using Eq. [1]. Data conforming to linear competitive, noncompetitive, and uncompetitive inhibition were fitted using Eqs. [2]–[4], respectively.

In Eqs. [1]–[4], v is the initial velocity, V is the maximum velocity, K_a is the K_m for reactant A, K_{is} and K_{ii} are inhibition constants for inhibitor I. In Eq. [5] Y is the value of the parameter of interest measured at any pH, C is the pH-independent value of Y, H is the concentration of H^+, and K_1 and K_2 are acid dissociation constants for enzyme groups.

Electron paramagnetic resonance spectroscopy. Normal-mode X-band EPR data were obtained on a Bruker EPR 200 D spectrometer. The microwave frequency of 100 kHz was measured with a Systron Donner frequency counter, Model 1292A. The modulation frequency was always 100 kHz. The amplitude of modulation was calibrated on the modulation broadening of the signal from the Bruker strong-pitch sample. The spectrometer was interfaced with a PC with software written in ASYST for 1024-point data acquisition, correction for background signals, double integration procedures, and g value determinations. The external standard for integration was 10 mM $CuSO_4$/10 mM HCl/2 M $NaClO_4$. Native enzyme (50 μl, 10.58 mg/ml) plus 50 μl 0.5 M Ches, pH 9.5, in the absence and presence of 1 mM uracil was reduced anaerobically with 5 μl 100 mM dithionite in Ches buffer, incubated for 10 min, and then immediately frozen.

Expression plasmid and growth of bacteria. The expression plasmid has been constructed in the vector pSE420 using the pig DPD cDNA previously subcloned into the vector pSPORT. The cDNA contains an *Nco*I site coincident with the start codon (CCATGG) which was joined to the *Nco*I site in the vector that is in frame with the bacterial initiator Met. The pig DPD cDNA was inserted into pSE420 as an *Nco*I/*Afl* III fragment from pSPORT (13).

A single colony from a freshly made transformation of *E. coli* DH5α cells with the expression vector was grown in 16 h to a stationary phase. Then, 10 ml of this

culture was allowed to grow in 1 liter of LB medium supplemented with 100 μM uracil, 100 μg ampicillin, 10 μM FAD, 10 μM FMN, 10 μM sodium sulfide, and 10 μM ferriammonium citrate at 30°C. After 90 min the trp-lac promoter of the expression system was induced by addition of 1 mM IPTG and the growth was continued for additional 48 h at 30°C with shaking. The bacteria were centrifuged at 6000*g* for 30 min and washed twice with 1 liter PBS. The yield is typically 4 g of wet paste per liter of culture medium.

Enzyme purification. The bacterial paste (40 g wet paste) was resuspended in 200 ml 35 mM potassium phosphate buffer, pH 7.3, containing 2.5 mM $MgCl_2$, 2 μM leupeptide, 0.1 mM PMSF, 1 mM benzamidine, 20 μM lysozyme, 10 mM EDTA, and 1 mM DTT. The bacterial cell walls were ruptured in a cell disruption bomb (Parr) at 4°C using nitrogen at 2200–2500 psi. Finally, the homogenate was centrifuged at 200,000*g* for 60 min resulting in the crude extract. The supernatant was subjected to an ammonium sulfate fractionation with a final saturation of 55%. The protein was pelleted and dissolved in buffer A (35 mM potassium phosphate buffer, pH 7.3, containing 2.5 mM $MgCl_2$ and 1 mM DTT) plus 1 mM benzamidine, 2 μM leupeptide, and 0.1 mM PMSF, and dialyzed against the same buffer to remove residual ammonium sulfate. The dialyzed protein was applied to a DEAE cellulose colum (5.0 $\times$ 10 cm) equilibrated with buffer A. Elution was accomplished with a KCl gradient 0–0.2 M (2 $\times$ 600 ml). The DPD active fractions were collected and concentrated in a Amicon pressure cell. The concentrated enzyme was then applied to a 2′,5′-ADP–Sepharose column (1.6 $\times$ 10 cm) equilibrated with buffer A. DPD was eluted with a KCl gradient 0–2.0 M (2 $\times$ 100 ml). Active fractions were combined and concentrated as described above.

RESULTS

Purification of the porcine recombinant enzyme. The purification of porcine recombinant DPD from *E. coli* was accomplished in three steps using an ammonium sulfate fractionation and a DEAE-cellulose and 2′,5′-ADP–Sepharose affinity column chromatography. The pure protein with a specific activity of 14.0 units/mg protein was obtained in 60.5% yield (Table 1). It is very stable even in very dilute solutions, which is in contrast to native pig DPD (6). Native gel electrophoresis revealed a molecular weight of the recombinant DPD of 214 kDA. The SDS/PAGE shows a single band corresponding to a molecular weight of 107 kDa (Fig. 1). In contrast to the pig liver DPD (6), no proteolytic degradation of the subunit was detected for the recombinant DPD. The isoelectric point determined by using the Phast system was found to be 4.8 (data not shown).

Iron, acid-labile sulfide, and flavin determination. Three determinations of iron gave 9.0 $\pm$ 0.2 mol/mol subunit and 12 determinations of acid-labile sulfide gave 8.0 $\pm$ 1.4 mol/mol subunit, indicating the presence of two [4Fe–4S] clusters/subunit. The flavin content was found to be 2.0 $\pm$ 0.3 mol FAD and 2.0 $\pm$ 0.2 mol FMN per dimer, respectively.

EPR studies. Native porcine recombinant DPD in 500 mM Ches buffer, pH 9.5, reduced with dithionite for 10 min gave at 16K an EPR spectrum with features at effective *g* values at 2.033, 2.012, 1.947, and 1.900 (Fig. 2). The complex spectral shape indicates the dipole–dipole interaction of two [4Fe–4S] clusters which are about 1 nm apart. Also the broadening of the EPR at temperatures of above 20K is consistent with the assignment to $[4Fe–4S]^{1+}$ ferredoxin-like cubanes. Increasing the pH above 9.5 during the reduction of DPD with dithionite did not increase the spin/subunit. Integration of the signal intensity revealed 0.95 spins per reduced subunit where 2 spins were expected (see Discussion).

Initial velocity studies in the absence of products. Kinetic studies were conducted with porcine recombinant DPD preparations having specific activities of 14 units/mg of protein. When the velocity was determined at various uracil concentrations and several fixed levels of NADPH, the initial velocity pattern in Fig. 3 was obtained. The pattern is composed of parallel lines at low reactant concentrations. Since the K_m values for both reactants are rather low, with $K_{\text{uracil}} = 1.0 \pm 0.1$ μM and $K_{\text{NADPH}} = 6.0 \pm 0.6$ μM, and are at the limits of detection of the recording spectrometer, data were also obtained in the presence of 2,6-DHP, an inhibitor that is noncompetitive versus uracil and NADPH (9). In the presence of 2,6-DHP, the K_m for uracil was now in a measurable range, and substrate inhibition by uracil and NADPH was eliminated. The parallel pattern shown in Fig. 3C gave calculated values of 6.6 $\pm$ 0.7 and 23 $\pm$ 1 μM for K_{NADPH} and K_{uracil}, respectively.

Product inhibition. $NADP^+$ was a linear competitive inhibitor versus NADPH at high ($50 \times K_{\text{uracil}}$) levels of uracil, whereas it was noncompetitive versus uracil. With variable NADPH as substrate, DHU was uncompetitive versus uracil. When the uracil concentration was varied, DHU was competitive at any NADPH concentration (data not shown). Results are summarized in Table 2.

Dead-end inhibition. Further information about the kinetic mechanism was obtained with dead-end analogues of the two substrates. ATP-ribose, a dead-end analogue of NADPH, was competitive versus NADPH, whereas uncompetitive inhibition was found versus uracil. When uracil was the variable substrate, 2,6-DHP, which is structurally related to uracil (16), was competitive with uracil and noncompetitive with

TABLE 1

Purification of Porcine Recombinant Dihydropyrimidine Dehydrogenase from *Escherichia coli* Starting with 40 g Wet Cell Paste

Purification step	Volume (ml)	Total protein (mg)	Total activity (units)	Specific activity (units/mg)	Yield (%)
Crude extract	250	12,400	552	0.04	100
Ammonium sulfate fractionation	31	1,961	508	0.3	92
DEAE-cellulose	15	790	460	0.6	83
2′,5′-ADP–Sepharose	46	23.8	334	14.0	60.5

NADPH (data not shown). Table 2 summarizes the dead-end inhibition data.

pH dependence of kinetic parameters. Kinetic parameters for the porcine recombinant DPD reaction were measured over the pH range 5.5–9.0. All pH profiles are quantitatively identical to those of native enzyme (data not shown). When NADPH concentrations were varied with uracil levels fixed at 20 μM or when uracil concentrations were varied with NADPH concentrations fixed at 60 μM, the value for V was observed to decrease at both low and high pH. V decreases from a constant value at pH 8 to a lower constant value around pH 7 and then decreases further with a pK of 6.0 ± 0.2. A decrease in V is also observed at high pH with a pK of about 9. V/K_{NADPH} obtained by varying the concentrations of NADPH at 20 μM uracil decreases at high and low pH giving pK values of 5.5 ± 0.5 and 8.4 ± 0.3, while V/K_{uracil} also decreases at high and low pH giving pK values of 5.8 ± 0.3 and 9.2 ± 0.3.

pH dependence of the dissociation constant of 2,6-dihydroxypyridine. The dissociation constant for 2,6-dihydroxypyridine, a competitive inhibitor of uracil, is slightly pH dependent, giving estimated pK values of 6 and 9 (data not shown), identical to data obtained for native enzyme (12). The pH-independent value for $K_{i(2,6DHP)}$ is 50 nM, within error identical to the value of 40 nM obtained for the native enzyme.

DISCUSSION

The pig liver DPD was expressed in *E. coli* DH-5α cells using the vector pSE420 which has a trp-lac promoter that is inducible by IPTG (13). Optimal expression was obtained when cells were grown at 30°C in LB medium supplemented with uracil, ampicillin, FAD,

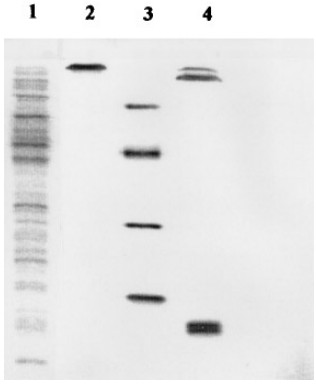

FIG. 1. SDS/PAGE of various purification steps of porcine recombinant dihydropyrimidine dehydrogenase. Lane 1, DEAE cellulose extract; lane 2, purified recombinant DPD; lane 3, bovine serum albumin (67 kDa), ovalbumin (43 kDa), chymotrysinogen A (25 kDa), and ribonuclease (13.7 kDa) (standard proteins); and lane 4, pig liver DPD (107, 92, and 12 kDa). The protein concentrations in lanes 2–4 were 0.2, 0.8, and 0.4 μg, respectively.

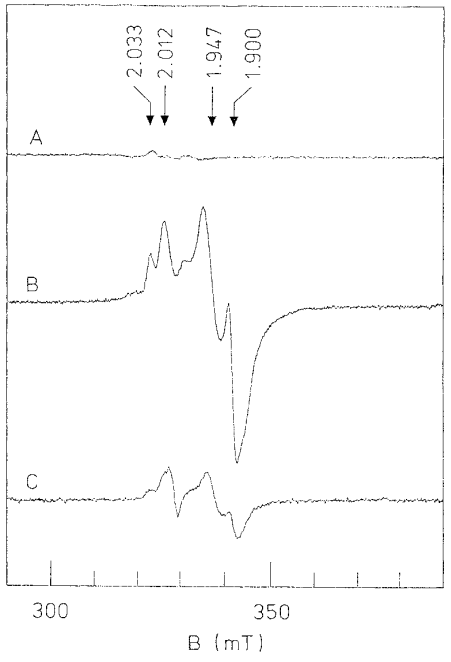

FIG. 2. EPR spectra of porcine recombinant dihydropyrimidine dehydrogenase. (A) Native enzyme (46 μM subunits) in 35 mM potassium phosphate, pH 7.4. (B) Dehydrogenase in 500 mM Ches, pH 9.5, reduced with 100 mM dithionite (10 mM final concentration) for 10 min. (C) The same as in B but in the presence of 1 mM uracil. The temperature was 16K, the microwave frequency was 9186 MHz, the microwave power was 2 (A) and 0.32 mW (B and C), the modulation frequency was 100 kHz, and the modulation amplitude was 1.0 mT.

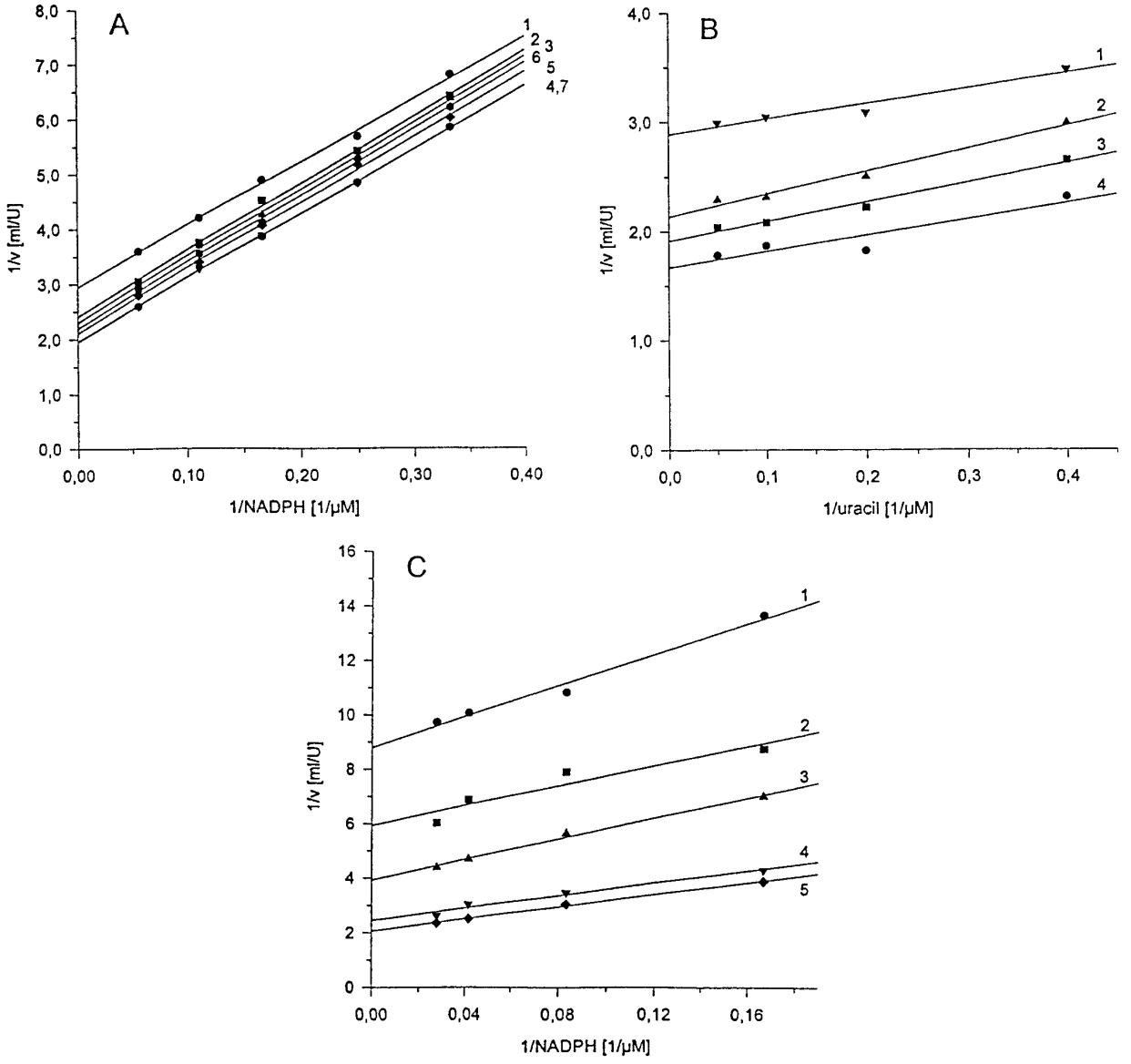

FIG. 3. Initial velocity pattern of NADPH and uracil. (A) 1/*v* versus 1/NADPH at different fixed concentrations of uracil (line 1, 2.5 μM; line 2, 3.0 μM; line 3, 5 μM; line 4, 10 μM; line 5, 20 μM; line 6, 100 μM; line 7, 500 μM); (B) 1/*v* versus 1/uracil at different fixed concentrations of NADPH (line 1, 12 μM; line 2, 36 μM; line 3, 60 μM; line 4, 240 μM); (C) 1/*v* versus 1/NADPH at different concentrations of uracil and in the presence of 0.5 μM 2,6-DHP (line 1, 5 μM; line 2, 10 μM; line 3, 20 μM; line 4, 100 μM; line 5, 500 μM).

FMN, sodium sulfide, and ferriammonium citrate. After 90 min the promoter of the expression system was induced by addition of IPTG (13).

Initially, porcine recombinant DPD was only partially purified by an ammonium sulfate fractionation of the crude extract (13). In this study we report the purification of porcine recombinant DPD to homogeneity. The crude extract is not obtained by sonification but by rupturing cell walls using a cell disruption bomb. The protein concentration of the crude extract is much higher than that obtained with sonification (B. Schaffrath, M.S. thesis). Pure porcine recombinant DPD is obtained after a 350-fold purification in twice the yield when compared to native pig DPD after a 3100-fold purification (6). The specific activity is slightly lower for the porcine recombinant dehydrogenase when compared with native pig enzyme (14 vs 21 units/mg). One reason for the difference is the lower temperature of the assay (30 vs 37°C) and another could be the different protein assays used. Noteworthy is the fact that the porcine recombinant dehydrogenase is much more stable even in more dilute solutions.

The EPR studies of reduced, porcine recombinant DPD show signals at 2.03, 2.01, 1.95, and 1.90*g*, respec-

TABLE 2

Summary of Product and Dead-End Inhibition Data for Porcine Recombinant Dihydropyrimidine Dehydrogenase at pH 7.3 and 30°C

Variable substrate	Fixed substrate[a]	Inhibitor	Pattern[b]	K_{is} ± SE (μM)	K_{ii} ± SE (μM)
Uracil	NADPH	$NADP^+$	NC	25 ± 8	32 ± 2
Uracil	NADPH	DHU	C	840 ± 290	—
NADPH	Uracil	$NADP^+$	C	1.0 ± 0.2	—
NADPH	Uracil	DHU	UC	—	24 ± 2
Uracil	NADPH	ATP-ribose	UC	—	1.0 ± 0.1
Uracil	NADPH	2,6-DHP	C	0.05 ± 0.01	—
NADPH	Uracil	ATP-ribose	C	25 ± 5	—
NADPH	Uracil	2,6-DHP	NC	0.13 ± 0.07	0.08 ± 0.01

[a] Fixed substrate was at a saturating concentration, that is, 5–20 times K_m.
[b] C, competitive; UC, uncompetitive; NC, noncompetitive.

tively, indicating dipole–dipole interactions between two [4Fe–4S] clusters in close proximity as commonly observed in two [4Fe–4S] ferredoxins (17) and in iron–sulfur enzymes, e.g., Fe-hydrogenase (18), and acetylCoA synthase (19). The signals are only equivalent to 0.95 spins per subunit, but 2 spins per subunit were expected. These results indicate that the redox potential of the Fe/S clusters in DPD is lower than −450 mV which is highly unusual since the reducing equivalents come from NADPH.

No differences in physicochemical parameters have been found for porcine recombinant and native dihydropyrimidine dehydrogenase, with the exception that the porcine recombinant DPD shows only a single band on SDS/PAGE. The latter indicates that there are no proteolytic degradation products in the preparation of the porcine recombinant DPD. All kinetic parameters are identical within error to those obtained for the native enzyme (9). All data are consistent with the porcine recombinant enzyme being identical in structure and mechanism to the native DPD.

ACKNOWLEDGMENTS

This study was supported by grants to P.F.C. from the National Institutes of Health (GM 36799) and to K.D.S. from the Deutsche Forschungsgemeinschaft (Schn 139/11-3) and by Grant CRG 900519 from the North Atlantic Treaty Organization Scientific Affairs Division to P.F.C. and K.D.S.

REFERENCES

1. Wasternack, C. (1980) Degradation of pyrimidines and pyrimidine analogs—Pathways and mutual influences. *Pharmacol. Ther.* **8,** 629–651.
2. Hull, W. E., Port, R. E., Herrmann, R., Britsch, B., and Kunz, W. (1988) Metabolites of 5-fluorouracil in plasma and urine, as monitored by ^{19}F nuclear magnetic resonance spectroscopy, for patients receiving chemotherapy with or without methotrexate pretreatmant. *Cancer Res.* **48,** 1680–1688.
3. Okeda, R., Shibutani, M., Matsuo, T., Kuroiwa, T., Shimokawa, R., and Tajima, T. (1990) Experimental neurotoxicity of 5-fluorouracil and its derivatives is due to poisoning by the monofluorinated organic metabolites, monofluoroacetic acid and α-fluoro-β-alanine. *Acta Neuropathol.* **81,** 66–73.
4. Ho, D. H., Towensend, L., Luna, M. A., and Bodely, G. P. (1986) Distribution and inhibition of dihydrouracil dehydrogenase activities in human tissues using 5-fluorouracil as a substrate. *Anticancer Res.* **6,** 781–784.
5. Shiotani, T., and Weber, G. (1981) Purification and properties of dihydrothymine dehydrogenase from rat liver. *J. Biol. Chem.* **256,** 219–224.
6. Podschun, B., Wahler, G., and Schnackerz, K. D. (1989) Purification and characterization of dihydropyrimidine dehydrogenase from pig liver. *Eur. J. Biochem.* **185,** 219–224.
7. Porter, D. J. T., Chestnut, W. G., Taylor, L. E. C., Merrill, B. M., and Spector, T. (1991) Inactivation of dihydropyrimidine dehydrogenase by 5-iodouracil. *J. Biol. Chem.* **266,** 19988–19994.
8. Lu, Z. H., Zhang, R., and Diasio, R. (1992) Purification and characterization of dihydropyrimidine dehydrogenase from human liver. *J. Biol. Chem.* **267,** 17102–17109.
9. Podschun, B. Cook. P. F., and Schnackerz, K. D. (1990) Kinetic mechanism of dihydropyrimidine dehydrogenase from pig liver. *J. Biol. Chem.* **265,** 12966–12972.
10. Podschun, B. (1992) Stereochemistry of NADPH oxidation by dihydropyrimidine dehydrogenase from pig liver. *Biochem. Biophys. Res. Commun.* **182,** 609–616.
11. Gani, D., and Young, D. W. (1985) Stereochemistry of catabolism of the RNA base uracil *J. Chem. Soc. Perkin Trans. I,* 1355–1362.
12. Podschun, B., Jahnke, K., Schnackerz, K. D., and Cook, P. F. (1993) Acid base catalytic mechanism of the dihydropyrimidine dehydrogenase from pH studies. *J. Biol. Chem.* **268,** 3407–3413.
13. Yokota, H., Fernandez-Salguerno, P., Furuya, H., Lin, K., McBride, O. W., Podschun, B., Schnackerz, K. D., and Gonzalez, F. J. (1994) cDNA cloning and chromosome mapping of human dihydropyrimidine dehydrogenase, an enzyme associated with 5-fluorouracil toxicity and congenital thymine uraciluria. *J. Biol. Chem.* **269,** 23192–23196.
14. Blum, H., Beyer, H., and Gross, H. J. (1987) Improved silver staining of plant proteins, RNA and DNA in polyacrylamide gels. *Electrophoresis* **8,** 93–99.

15. Cleland, W. W. (1979) Statistical analysis of enzyme kinetic data. *Methods Enzymol.* **63,** 103–138.
16. Tatsumi, K., Fukushima, M., Shirasaka, T., and Fujii, S. (1987) Inhibitory effects of pyrimidine, barbituric acid and pyridine derivatives on 5-fluorouracil degradation in rat liver extracts. *Jpn. J. Cancer Res. (Gann)* **78,** 748–755.
17. Mathews, R., Charlton, S., Sands, R. H., and Palmer, G. (1974) On the nature of the spin coupling between the iron–sulfur cluster in the eight-iron ferrodoxins. *J. Biol. Chem.* **249,** 4326–4328.
18. Grande, H. J., Dunham, W. R., Averill, B., van Dijk, C., and Sands, R. H. (1983) Electron paramagnetic resonance and other properties of hydrogenases isolated from Desulfovibrio vulgaris (strain Hildenborough) and Megasphaera elsdenii. *Eur. J. Biochem.* **136,** 201–207.
19. Jetten, M. S. M., Hagen, W. R., Pierik, A. J., Stams, A. J. M., and Zehnder, A. J. B. (1991) Paramagnetic centers and acetyl-coenzyme A/CO exchange activity of carbon monoxide dehydrogenase from Methanothrix soehngenii. *Eur. J. Biochem.* **195,** 385–391.